

Tidal flow field in a small basin

Sergio Fagherazzi

Department of Geological Sciences and School of Computational Science and Information Technology, Florida State University, Tallahassee, Florida, USA

Patricia L. Wiberg and Alan D. Howard

Department of Environmental Sciences, University of Virginia, Charlottesville, Virginia, USA

Received 11 February 2002; revised 27 November 2002; accepted 27 December 2002; published 13 March 2003.

[1] The tidal flow field in a basin of small dimensions with respect to the tidal wavelength is calculated. Under these conditions, the tide becomes a standing wave oscillating synchronously (with a flat water surface) over the whole basin. The shallow water equations can thus be strongly simplified, expressing the discharge vector field in terms of a potential function and a stream function. The potential function can be independently solved with the continuity equation, and is responsible for the total water balance in the basin. Moreover, the flow field derived from the potential function is shown to represent the tidal motion in a deep basin with flat bottom. Departures from this situation are treated with a stream function, that is, a correction for the potential function solution, and is solved through the vorticity equation. The stream function accounts for the nonlinear inertial terms and the friction in the shallow water equations, as well as bottom topography. In basins where channels incise within shallow tidal flats, the solution demonstrates that friction redistributes momentum, increasing the flow in the channels and decreasing it on the flats. The model is tested in San Diego Bay, California, with satisfactory results.

INDEX TERMS: 4560 Oceanography: Physical: Surface waves and tides (1255); 4203 Oceanography: General: Analytical modeling; 4235 Oceanography: General: Estuarine processes; 4255 Oceanography: General: Numerical modeling; *KEYWORDS:* tides, tidal channel, tidal flow, tidal velocity

Citation: Fagherazzi, S., P. L. Wiberg, and A. D. Howard, Tidal flow field in a small basin, *J. Geophys. Res.*, 108(C3), 3071, doi:10.1029/2002JC001340, 2003.

1. Introduction

[2] The oscillatory motion of the tide in a lagoon produces water fluxes inside the basin and at the inlets that are of fundamental importance for several nearshore processes. For example, from a geomorphic point of view, the tidal flow is the main force responsible for the creation and evolution of dendritic channels that often dissect tidal flats and salt marshes. Clearly the tidal flow is determinant for the sediment budget and the dispersion of contaminants in shallow lagoons, and its correct modeling becomes crucial in assessing an eventual environmental risk.

[3] A powerful and widely used technique for the determination of tidal fluxes in a basin is based on the numerical resolution of the shallow water equations, given the basin shape and tidal characteristics. The numerical resolution of this problem, accomplished with several refined methods [see Velyan, 1992], yields to results of remarkable precision, when compared to measured tidal velocities [e.g., Wang *et al.*, 1998]. However, in determined situations, a correct analysis of the equations and the application of suitable simplifications that enhance the leading terms can be of great scientific interest and provide simplified but physi-

cally based tools for different important applications. In the context of tidal basins it is natural to wonder what is the influence of the basin shape on the tidal flow, and whether it is possible to separate this influence from the effect of the basin bottom topography.

[4] This paper shows that, under precise hypotheses, it is possible to split the tidal flow in a component dependent on the basin shape and a component dependent on the basin bottom topography. This mathematical development is not only a mere exercise, but opens the door to physical applications of great interest. In cases where the bathymetry of tidal basins is not available, say for example when remote sensing data are used, a simplified method that estimates the tidal discharge within the basin, neglecting the bathymetry, becomes helpful. Clearly we are also interested in knowing what correction we need to add to this solution in order to obtain realistic discharges with different bottom configurations. Furthermore, the basin boundaries and the basin bottom are features of the coastal landscape that evolve at different timescales. The boundaries, often determined by the shape of river paleo-valleys, usually vary with sea level oscillations, i.e., in thousands of years. On the other hand, the basin bottom is modified by several agents, including for example a change in the sediment input from rivers and the dredging of channels for navigation, that typically act at a smaller timescale, from decades to centuries. Thus a

method able to separate the component of the flow field due to the basin shape from the component determined by the bottom topography results straightforward in studying the short term evolution of tidal basins and their channel networks.

[5] When the tide enters a basin of limited dimensions, the signal is reflected at the mainland boundaries, and the tide assumes characteristics of a standing wave, with strong currents around mid-tide and minimum velocity at high and low water (slack water) [Wright *et al.*, 2000].

[6] The fact that in small basins the tidal wave is similar to a standing wave was pointed out by Schuttelaars and De Swart [2000], as compared with the progressive character of the tide in a large estuary [Lanzone and Seminara, 1998; Friedrichs and Aubrey, 1994]. In a small basin an intuitive approach is to consider water elevation to be flat and oscillating synchronously with the tide at the inlet. This assumption is common in classical studies of tidal inlets, where the tidal basin is treated as a reservoir with oscillating elevation and the flow along the inlet is calculated by means of open channel hydraulics [Bruun, 1978].

[7] Schuttelaars and De Swart [1996] showed that, for small tidal basins, the tidal wavelength is long with respect to the basin dimensions, so that the water surface can be considered flat as a first approximation (i.e., the phase difference in different locations of the basin is negligible and the water surface is oscillating synchronously everywhere). This hypothesis has been previously utilized to calculate the discharge [Boon, 1975] and to explain the velocity asymmetry [Pethick, 1980] in salt marsh creeks. Healey *et al.* [1981] questioned the applicability of this simplification in salt marshes, and Rinaldo *et al.* [1999b] showed that discrepancies arise from the complex nonlinear phenomenon of wetting and drying of the marsh surface. The same hypothesis of a flat surface was adopted to study the equilibrium bottom configuration in a rectangular tidal basin [Schuttelaars and de Swart, 1999], to single out the drainage area of salt marsh creeks [Rinaldo *et al.*, 1999a], and to model the cross-sectional evolution of marsh channels [Fagherazzi and Furbish, 2001].

[8] Even though the hypothesis of basin dimensions small with respect to the tidal wavelength (hereinafter referred to as “small embayment hypothesis”) and the consequent flat water surface has already been utilized in different studies, there is an evident need to develop in detail the simplifications that this hypothesis yields to the tidal flow. We will first present the simplified unidimensional formulation that allows us to understand the basic concepts; the rest of the paper is then the extensions of the same concepts to the full bidimensional shallow water equations.

[9] In shallow water the unidimensional propagation of a wave of small amplitude can be formulated with two equations, continuity and conservation of linear momentum [Stoker, 1957, p. 24],

$$\frac{\partial \eta}{\partial t} = -h \frac{\partial u}{\partial x}, \quad (1a)$$

$$\frac{\partial u}{\partial t} = -g \frac{\partial h}{\partial x}, \quad (1b)$$

with η the water surface elevation with respect to Mean Sea Level (M.S.L.), h the depth of the bottom with respect to

M.S.L., u the water velocity averaged over the vertical, g the gravity acceleration, t time and x the space coordinate. Equations (1a) and (1b) were derived considering an incompressible fluid, eliminating inertial and diffusion terms, neglecting the friction at the bottom and averaging the unidimensional equations over the vertical direction. A sinusoidal tidal wave traveling in one direction in an unconfined domain is then governed by the two following equations, derived from equation (1):

$$\begin{aligned} \eta &= a \sin \omega \left(t - \frac{x}{c} \right) \\ u &= c \sin \omega \left(t - \frac{x}{c} \right), \end{aligned} \quad (2)$$

where a is the wave amplitude, ω is the angular frequency, and $c = \sqrt{gh}$ the wave celerity in shallow water. Both surface elevation and velocity vary in space and time, but they are in phase, in the sense that u and η simultaneously reach their maximum at a given time. Moreover the velocity u scales with $c = \omega\lambda$, where λ is the tidal wavelength. On the contrary, if the tidal wave reaches an obstacle, say a vertical wall, it gets reflected, forming a standing wave. The equations for the standing wave, obtained by summing two waves given by equation (2) traveling in opposite directions, are

$$\begin{aligned} \eta &= 2a \sin \omega t \cos \frac{\omega}{c} x \\ u &= 2c \cos \omega t \sin \frac{\omega}{c} x, \end{aligned} \quad (3)$$

where now x is the distance from the wall. In this case the surface elevation and the velocity are out of phase, with the maximum of velocity occurring for zero elevation and vice versa. At a distance L from the wall small with respect to the wavelength then $\omega L/c = L/\lambda$ is small and the approximations $\cos \frac{\omega}{c} L \sim 1$ and $\sin \frac{\omega}{c} L \sim \frac{\omega}{c} L$ hold. Equation (3) then becomes

$$\begin{aligned} \eta &= 2a \sin \omega t \\ u &= 2\omega L \cos \omega t, \end{aligned} \quad (4)$$

with the velocity proportional to $L\omega$. The same equations are obviously valid for each point closer to the wall. Consequently, equation (4) show that for $x < L$ the water elevation is flat and oscillates synchronously with the tide, whereas the velocity decreases proportionally to the distance from the wall, going to zero for $L = 0$.

2. Shallow Water Equations

[10] The barotropic tidal motion in a well mixed basin is described by the two-dimensional shallow water equations. This system of equations is derived from the Reynolds equations after vertical integration, with the hypothesis of hydrostatic pressure distribution along the vertical [Pedlosky, 1987, p. 59]. In conservative form the equations read

$$\frac{\partial \eta^*}{\partial t^*} + \frac{\partial q^*}{\partial x^*} + \frac{\partial p^*}{\partial y^*} = 0 \quad (5)$$

$$\begin{aligned} \frac{\partial q^*}{\partial t^*} + \frac{\partial}{\partial x^*} \left(\frac{q^{*2}}{h^* + \eta^*} \right) + \frac{\partial}{\partial y^*} \left(\frac{q^* p^*}{h^* + \eta^*} \right) \\ = -g(h^* + \eta^*) \frac{\partial \eta^*}{\partial x^*} - C_f (q^{*2} + p^{*2})^{1/2} \frac{q^*}{(h^* + \eta^*)^2} \end{aligned} \quad (6)$$

$$\begin{aligned} \frac{\partial p^*}{\partial t^*} + \frac{\partial}{\partial x^*} \left(\frac{q^* p^*}{h^* + \eta^*} \right) + \frac{\partial}{\partial y^*} \left(\frac{p^{*2}}{h^* + \eta^*} \right) \\ = -g(h^* + \eta^*) \frac{\partial \eta^*}{\partial y^*} - C_f (q^{*2} + p^{*2})^{1/2} \frac{p^*}{(h^* + \eta^*)^2}, \end{aligned} \quad (7)$$

where q^* and p^* are the discharges per unit width in the x and y direction, C_f a friction coefficient, η^* and h^* the elevation of the water surface and the water depth with respect to M.S.L. (for fixed bottom h^* does not vary in time). Herein the asterisk indicates dimensional quantities. Introducing a scale H for the water depth, a length scale L , a scale ω for the tidal angular frequency, and a velocity scale U , the quantities in equations (5), (6), and (7) are nondimensionalized with

$$\begin{aligned} h^* = Hh, \quad \eta^* = H\eta, \quad t^* = t/\omega, \quad x^* = xL, \\ y^* = yL, \quad p^* = UHp, \quad q^* = Uhq, \end{aligned} \quad (8)$$

where p , q , h , η , t , x , y are the corresponding nondimensional quantities. For traveling tidal waves the length scale L is the wavelength [Prandle, 1991]. On the contrary, in a limited basin, the tidal motion is constrained by the proximity of the reflecting boundaries. The length scale L is then the distance from the mainland, or, as expressed here, the basin dimension.

[11] After nondimensionalization, the continuity equation (5) becomes

$$\frac{\partial \eta}{\partial t} + \frac{U}{L\omega} \left(\frac{\partial q}{\partial x} + \frac{\partial p}{\partial y} \right) = 0. \quad (9)$$

Since the variations in water elevation have to be balanced by the divergence of the water discharge, it follows that $U \sim L\omega$. This corresponds to equation (4), and shows that the velocity in proximity of a reflecting boundary is proportional to the distance from the boundary itself. Applying this scaling to the nondimensional equations results in

$$\frac{\partial \eta}{\partial t} + \frac{\partial q}{\partial x} + \frac{\partial p}{\partial y} = 0 \quad (10)$$

$$\begin{aligned} \epsilon \left[\frac{\partial q}{\partial t} + \frac{\partial}{\partial x} \left(\frac{q^2}{h + \eta} \right) + \frac{\partial}{\partial y} \left(\frac{qp}{h + \eta} \right) \right] \\ = -(h + \eta) \frac{\partial \eta}{\partial x} - \epsilon \Lambda (q^2 + p^2)^{1/2} \frac{q}{(h + \eta)^2} \end{aligned} \quad (11)$$

$$\begin{aligned} \epsilon \left[\frac{\partial p}{\partial t} + \frac{\partial}{\partial x} \left(\frac{qp}{h + \eta} \right) + \frac{\partial}{\partial y} \left(\frac{p^2}{h + \eta} \right) \right] \\ = -(h + \eta) \frac{\partial \eta}{\partial y} - \epsilon \Lambda (q^2 + p^2)^{1/2} \frac{p}{(h + \eta)^2}, \end{aligned} \quad (12)$$

where the two nondimensional parameters ϵ and Λ are

$$\epsilon = \frac{\omega^2 L^2}{gH}, \quad \Lambda = C_f \frac{L}{H}. \quad (13)$$

The parameter ϵ is the squared ratio of the time it takes for a long wave in shallow water to travel along the basin (L/\sqrt{gH}) to the tidal period ($1/\omega$). The parameter Λ measures the relative importance of the friction in the specific basin. A small value of ϵ implies a tidal wave traveling at a fast speed and a water level almost in phase at every point in the basin. Since the period of the tidal wave is very long (12 or 24 hours), in basins of limited dimensions, the tidal wave can be considered in phase everywhere. Herein the basin dimensions are considered to be small, so that L is negligible with respect to the tidal wavelength. In this case the terms of order ϵ can be neglected in equations (10), (11), and (12). Under this simplification, equations (11) and (12) reduce to $\partial \eta / \partial x = 0$ and $\partial \eta / \partial y = 0$, respectively, showing that the water surface is flat and its elevation equal to the value of the oscillating elevation at the inlet ($\eta(t) = \eta_{inlet}(t)$). Only equation (10) remains for the determination of the two variables q and p , and the system is undetermined. To obtain a solution, equations (10), (11), and (12) are rewritten in terms of vorticity, subtracting the derivative with respect to x of the third equation from the derivative with respect to y of the second equation, thus eliminating the derivatives of the water surface elevation η [Zimmerman, 1978]. Another equation springs from the sum of the x -derivative of the second equation and y -derivative of the third equation. After elimination of the terms in ϵ , the new system is

$$\frac{\partial \eta_0}{\partial t} + \nabla \cdot \mathbf{q}_0 = 0 \quad (14)$$

$$\begin{aligned} \frac{\partial \Omega_0}{\partial t} + \left(\frac{\mathbf{q}_0}{h_0 + \eta_0} \cdot \nabla \right) \Omega_0 = \frac{\Omega_0}{h_0 + \eta_0} \left[\frac{\partial \eta_0}{\partial t} + \frac{\mathbf{q}_0}{h_0 + \eta_0} \cdot \nabla h_0 \right] \\ - \nabla \times \left[\Lambda \frac{|\mathbf{q}_0|}{(h_0 + \eta_0)^3} \mathbf{q}_0 \right] \end{aligned} \quad (15)$$

$$\nabla^2 \eta_0 = 0, \quad (16)$$

where the vector of the discharge per unit width \mathbf{q}_0 and the vorticity Ω_0 are, respectively

$$\mathbf{q}_0 = (q_0, p_0), \quad \Omega_0 = \nabla \times \frac{\mathbf{q}_0}{h_0 + \eta_0}, \quad (17)$$

with the subscript 0 indicating that the system has been determined neglecting the terms of $O(\epsilon)$. The two systems (equations (14), (15), and (16) without the terms of order ϵ) and equations (10), (11), and (12) are equivalent if no part of the basin floor dries during the tidal cycle and if the water depth and the discharge per unit width are continuous with continuous derivatives [Courant and Hilbert, 1953].

3. Potential and Stream Function

[12] To solve equations (14), (15), and (16) the vector field $\mathbf{q}_0 = (q_0, p_0)$ is rewritten as the sum of two new vector fields, one irrotational (zero curl), and one solenoidal (zero divergence) [Batchelor, 1967]. The transformation has general validity, since any vector field can be split in this way [Jeffreys and Swirles, 1972]. After introduction of a poten-

tial function Φ for the irrotational field and a stream function Ψ for the solenoidal field, the discharge per unit width is rewritten as

$$q_0 = \frac{\partial \Phi}{\partial x} + \frac{\partial \Psi}{\partial y}, \quad p_0 = \frac{\partial \Phi}{\partial y} - \frac{\partial \Psi}{\partial x}. \quad (18)$$

In vectorial form, introducing a potential vector $\mathbf{B} = (0, 0, \Psi)$, equation (18) reads

$$\mathbf{q}_0 = \nabla \Phi + \nabla \times \mathbf{B}. \quad (19)$$

Substitution of equation (19) into equation (14) leads to the following Poisson equation in Φ [Fagherazzi, 2002]:

$$\nabla^2 \Phi = -\frac{d\eta_0}{dt}, \quad (20)$$

while substitution of equation (19) into equation (15) gives a partial differential equation linking Ψ , Φ and η_0 ,

$$\begin{aligned} \frac{\partial \Omega_0}{\partial t} + \left(\frac{\nabla \Phi + \nabla \times \mathbf{B}}{h_0 + \eta_0} \cdot \nabla \right) \Omega_0 \\ = \frac{\Omega_0}{h_0 + \eta_0} \left[\frac{\partial \eta_0}{\partial t} + \frac{\nabla \Phi + \nabla \times \mathbf{B}}{h_0 + \eta_0} \cdot \nabla h_0 \right] \\ - \nabla \times \left[\Lambda \frac{|\nabla \Phi + \nabla \times \mathbf{B}|}{(h_0 + \eta_0)^3} (\nabla \Phi + \nabla \times \mathbf{B}) \right], \end{aligned} \quad (21)$$

where the vorticity Ω_0 expressed in terms of the potential function and potential vector is

$$\Omega_0 = \frac{\nabla^2 \Psi}{h_0 + \eta_0} - \frac{1}{(h_0 + \eta_0)^2} \nabla \times h_0 \cdot (\nabla \Phi + \nabla \times \mathbf{B}). \quad (22)$$

[13] Under the hypothesis of small embayment, the shallow water equations are then reduced to the two equations ((20) and (21)) plus the water elevation as a function of time. The advantages of this formulation are many. Only two unknowns (Φ , Ψ) remain instead of the original three unknowns (q , p , η), since the water elevation is everywhere equal to the elevation at the inlet. The value of Φ is calculated directly from equation (20), and it is independent of Ψ . Moreover, equation (20) is linear and allows the superposition of the results for each tidal harmonic. The potential function Φ depends on the value of $d\eta_0/dt$ at the instant in consideration, and it is not related to the flow field at other instants of the tidal cycle. Once Φ is calculated, the stream function Ψ is derived from equation (21). The stream function is nonlinear, so that Ψ cannot be calculated for each harmonic separately, and the solution at the time under consideration is intrinsically linked to the past solution. The system (equations (20) and (21)) can be readily applied in basins with many codominant tidal components. First the potential function derived from the linear equation (20) is calculated for every tidal component. Then the different solutions are added up to form the total potential function, and equation (21) is solved with $\Phi = \sum \Phi_i$.

[14] With the introduction of a potential function and a stream function, the solution is separated into two parts, each bearing different characteristics of the flow field. The potential function, determined through the continuity equation, accounts for the mass balance in the basin, and is responsible for the exchange of water volume with the ocean. It does not depend on bottom elevation, but only on the area and shape of the basin, which, under the hypothesis of flat water surface, are responsible for the total mass balance. The solution based on the stream function, with zero divergence, does not modify the amount of water entering in the basin, but redistributes momentum (discharge per unit width) taking into account bottom friction and inertia. As will be seen later, the depth distribution strongly influences the stream function and related flow field.

[15] In order to solve equations (20) and (21), suitable boundary conditions must be specified. At the border with the mainland (boundary Γ_1), the water flux is set to zero. The no-flux condition is expressed as $\frac{\partial \Phi}{\partial n} = 0$ and $\frac{\partial \Psi}{\partial r} = 0$, where n and r are the normal and tangent vector to the boundary. In particular, the condition $\frac{\partial \Psi}{\partial r} = 0$ along the boundary implies that the stream function has to be constant on it. It thus can be set to zero, since adding an arbitrary constant to Ψ and Φ does not affect the solution. At the basin inlets (boundary Γ_2), the discharge normal to the inlet cross section is exactly calculated from equation (20), knowing the water surface variation inside the basin. However, at the inlet boundary the value of the discharge in the direction tangent to the inlet cross section must be specified. In general this flux depends on the inlet shape and interaction with the ocean. Herein it is assumed that the discharge is always perpendicular to the inlet cross section (zero tangent discharge). Hence along the inlet, $\frac{\partial \Psi}{\partial n} = 0$ and $\frac{\partial \Phi}{\partial r} = 0$. As for Ψ at the mainland boundaries, Φ is set to zero at the inlet. The b.c. then become

$$\begin{aligned} \frac{\partial \Phi}{\partial n} = 0, \quad \Psi = 0 \quad \text{on } \Gamma_1 \\ \Phi = 0, \quad \frac{\partial \Psi}{\partial n} = 0 \quad \text{on } \Gamma_2, \end{aligned} \quad (23)$$

with n the normal direction to the boundary directed inward.

4. Small Oscillations Hypothesis

[16] To solve the bidimensional shallow water equations, a common simplification considers the wave amplitude to be small with respect to the water depth, allowing the treatment of nonlinear terms with perturbation techniques [Stoker, 1957]. This approach is based on the general framework of small oscillations around an equilibrium configuration of a physical system, where, in our case, the equilibrium configuration is represented by still water in the basin (a tidal amplitude approaching zero corresponds to no motion). It is important to stress that this hypothesis is independent of the hypothesis of basin of small dimensions with respect to the tidal wavelength, even though the two can be utilized simultaneously [Schuttelaars and De Swart, 1999].

[17] With the aim of shedding light on the structure of the system (equations (20) and (21)), the assumption is made that the tidal oscillation is small compared to the water

depth. The water elevation can then be rescaled with the tidal amplitude a ,

$$\eta^* = a\eta = \chi H\eta, \quad \text{with } \chi = \frac{a}{H}, \quad (24)$$

where the parameter χ represents the ratio between the tidal amplitude and the water depth (for small oscillations $\chi \rightarrow 0$). Substituting the new scaled variables in the continuity equation (5), the velocity scale becomes $U = \chi\omega L$, showing that for small oscillations the velocity is $O(\chi)$. The vorticity equation (15) becomes

$$\frac{\partial\Omega_0}{\partial t} + \chi \left(\frac{\mathbf{q}_0}{h_0 + \eta_0} \cdot \nabla \right) \Omega_0 = \frac{\Omega_0}{h_0 + \eta_0} \left[\chi \frac{\partial\eta_0}{\partial t} + \chi \frac{\mathbf{q}_0}{h_0 + \eta_0} \cdot \nabla h_0 \right] - \nabla \times \left[\chi \Lambda \frac{|\mathbf{q}_0|}{(h_0 + \eta_0)^3} \mathbf{q}_0 \right]. \quad (25)$$

Both the convective inertial term and the friction term are proportional to the square of the velocity, and can thus be neglected. Elimination of the terms of $O(\chi)$ in (25) yields

$$\frac{\partial\Omega_0}{\partial t} = 0. \quad (26)$$

Moreover, supposing that the bottom elevation is constant, substitution of equation (18) into equation (26) yields

$$\frac{\partial}{\partial t} (\nabla^2 \Psi) = 0 \quad (27)$$

This, together with the b.c. (equation (24)), leads to the result $\Psi = 0$. This means that for small oscillations and flat basin bottoms, the discharge per unit width is irrotational and the potential function is sufficient for calculating the flow field. Consequently, as already indicated by *Fagherazzi* [2002], the solution derived from the potential function represents the tidal motion in deep basins with flat bottom and weak friction, where the small oscillations hypothesis holds.

5. Basin Friction Dominated

[18] For shallow estuaries, *LeBlond* [1978] showed that frictional forces exceed acceleration over most of the tidal cycle, and thus cannot be ignored. Utilizing the same concept, *Friedrichs and Madsen* [1992] analyzed the generation of overtides from the nonlinear diffusion equation determined by neglecting the inertial terms and balancing friction with gravity in the De Saint Venant equations. In the context of tidal motion in a small basin, the motion can be considered frictionally dominated when $\Lambda \gg 1$ and $\epsilon\Lambda \ll 1$. The first condition assures that the friction term dominates the inertial terms, whereas the second condition is necessary for the hypothesis of small basin and flat water surface. If this is the case, the friction term is not able to balance the gravity term, as formulated by *LeBlond* [1978] and *Friedrichs and Madsen* [1992], and the flat water surface approximation is still valid. At the same time, a large friction term makes it possible to neglect the inertial terms in the vorticity equation (21), which reduces to

$$\nabla \times \left[\frac{|\nabla\Phi + \nabla \times \mathbf{B}|}{(h_0 + \eta_0)^3} (\nabla\Phi + \nabla \times \mathbf{B}) \right] = 0. \quad (28)$$

This nonlinear equation can be utilized to derive the stream function from the potential function at each instant of the tidal cycle. Because time derivatives are not involved, the solution does not depend on the solution at other instants of the tidal cycle. The parameter Λ does not appear in equation (28) because only the relative value of the frictional term between two different locations is important, rather than the absolute value of the friction itself. The parameter Λ instead plays a role when the frictional term is comparable to the inertial terms. However, in the part of the tidal cycle near slack water, when velocities are negligible, inertial terms are important, and their elimination becomes questionable. The three hypotheses, (1) basin of small dimensions, (2) small amplitude of the tidal oscillation, and (3) basin frictionally dominated, are independent of each other, and their application depends upon the geometric and dynamic characteristics of the tidal basin. In particular, the splitting of the discharge in a potential function component and in a stream function component is always valid if the basin has small dimensions, even for tidal amplitudes comparable to water depths. The small oscillation hypothesis was only introduced to give a physical meaning to the potential function solution, but this solution exists even if the water depths are small and the bottom is uneven. In the same way, the hypothesis of basin friction dominated was introduced to further simplify the vorticity equation (21), but the stream function solution is also valid in basins where the friction does not dominate. In the examples reported in the next section, equation (28) is adopted, since we consider small embayments friction dominated. That does not alter the fact that the same method can be applied to basins with weak friction, substituting equation (28) with equation (21).

6. Results

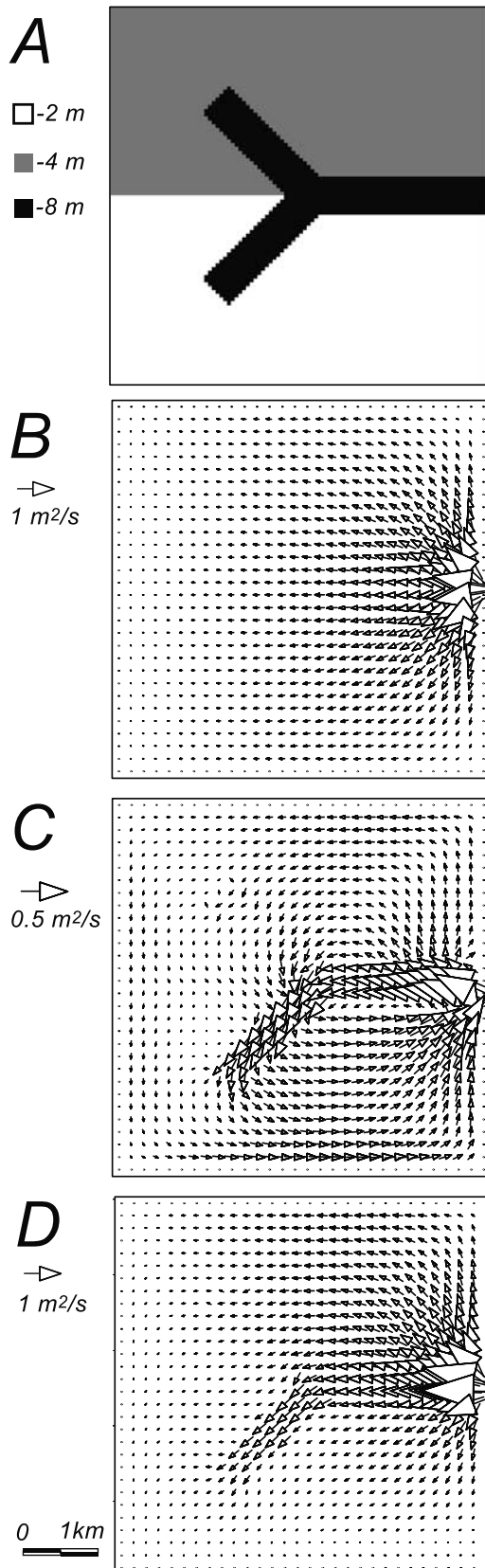
[19] As a test example, the method is applied to a schematic squared basin with a sinusoidal tidal signal with amplitude 52 cm and period 12.42 hours. The basin is 5 km wide, and a tidal inlet is situated in the middle of the right side (Figure 1a). A channel 8 m deep departs from the inlet and branches inside the basin in two separate channels that end in tidal flats having water depth of 4 m and 2 m, respectively (Figure 1a). Assuming a friction coefficient $C_f = 0.0023$ and an average water depth $H = 4$ m, the representative nondimensional parameters become $\epsilon = 0.009$, $\Lambda = 2.3$. Since ϵ is small, the small embayment theory can be utilized. Also, while $\epsilon\Lambda \ll 1$, $\Lambda > 1$, so that friction dominates the inertial terms. As a first approximation, equation (28) can be utilized instead of equation (21).

[20] The numerical scheme utilized to solve equation (28) is a finite difference method. Since equation (28) is nonlinear, the discharge module $|\nabla\Phi + \nabla \times \mathbf{B}|$ is set to one for the first iteration. Equation (28) is then solved discretizing $(\nabla\Phi + \nabla \times \mathbf{B})$ with central differences and solving the resulting linear system with a preconditioned biconjugate gradient method, since the corresponding matrix is not symmetrical. Then the term $|\nabla\Phi + \nabla \times \mathbf{B}|$ is updated with the new solution values and equation (28) solved a second time to derive a new approximation for the stream function Ψ . The method is repeated until convergence.

[21] We focus our attention on the maximum discharge field, when dh_0/dt is maximum.

$$h = a \sin(\omega t); \left. \frac{dh_0}{dt} \right|_{max} = a\omega = 7.255 \cdot 10^{-5} \text{ m/s}, \quad (29)$$

where a is the tidal amplitude and ω the angular frequency.



[22] The portion of the flow calculated from the potential function shows the typical vector field of a source point, with the source corresponding to the inlet and the discharge vectors with a sunburst pattern (Figure 1b). The stream function portion of the discharge redistributes momentum from the tidal flats to the channels, particularly for the lower branch, where the elevation difference between tidal flats and channel is higher. On the contrary the upper channel has less influence on the tidal flow (Figure 1c). The total discharge field shows a concentrated flux in the central and lower channel and a uniform discharge in the upper part of the basin (Figure 1d). The competition between channels is then in favor of the most incised ones, that convoy the highest water volume.

[23] The second example utilizes a squared basin with two islands located in the middle and the same tidal forcing of the first example (Figure 2a). The bottom elevation is constant in the basin, a part from a deep channel departing from the inlet. The same hypotheses, small embayment and basin friction dominated, are valid for this example as well. The presence of the islands modifies the potential function portion of the flow field, characterized by currents wrapping the two islands that provide water to the whole basin (Figure 2b). The channel has a local influence on the tidal flow, but does not considerably change the fluxes in the zones far from the inlet (Figures 2c and 2d). The splitting of the flow field presented herein is thus valid even when complex boundaries, islands, and multiple inlets are present.

[24] In the third example the method is applied to San Diego Bay, California (Figure 3a). San Diego Bay is a tidal basin connected to the Pacific Ocean by an inlet with an artificial jetty that controls beach erosion. Since freshwater flow in the bay is low, as is the average wind magnitude, currents are predominantly produced by tides [Wang *et al.*, 1998]. The astronomical tide in San Diego Bay is mixed, with the amplitude of the semidiurnal component M2 equal to 52 cm (period 12.42 hours) and the amplitude of the diurnal component K1 equal to 35 cm (period 23.93 hours) [Wang *et al.*, 1998]. The bathymetry of the bay shows the presence of a channel that extends from the inlet through the southern part of the bay, cutting the bay bottom close to the eastern boundaries, in front of the city port (Figure 3b).

[25] The hypothesis of a flat water surface is particularly valid for a small embayment with deep bottom. If the surface of the basin is limited, then the time spent by the tidal wave to propagate from the inlet to the extreme boundaries is negligible with respect to the tidal period, and the water surface is almost in phase everywhere. On the contrary, bottom friction in shallow areas reduces the tidal wave speed and attenuates the tidal peak as a consequence of energy dissipation. In San Diego Bay the phase shift between the inlet and the extreme boundaries is only 8 min for the M2 tidal component [Wang *et al.*, 1998], thus

Figure 1. (opposite) (a) Schematic tidal basin with incised channels and tidal flats having different water depths. (b) Component of the maximum flood discharge calculated from the potential function. (c) Component of the maximum flood discharge calculated from the stream function. (d) Total maximum flood discharge (sum of the potential and stream solutions).

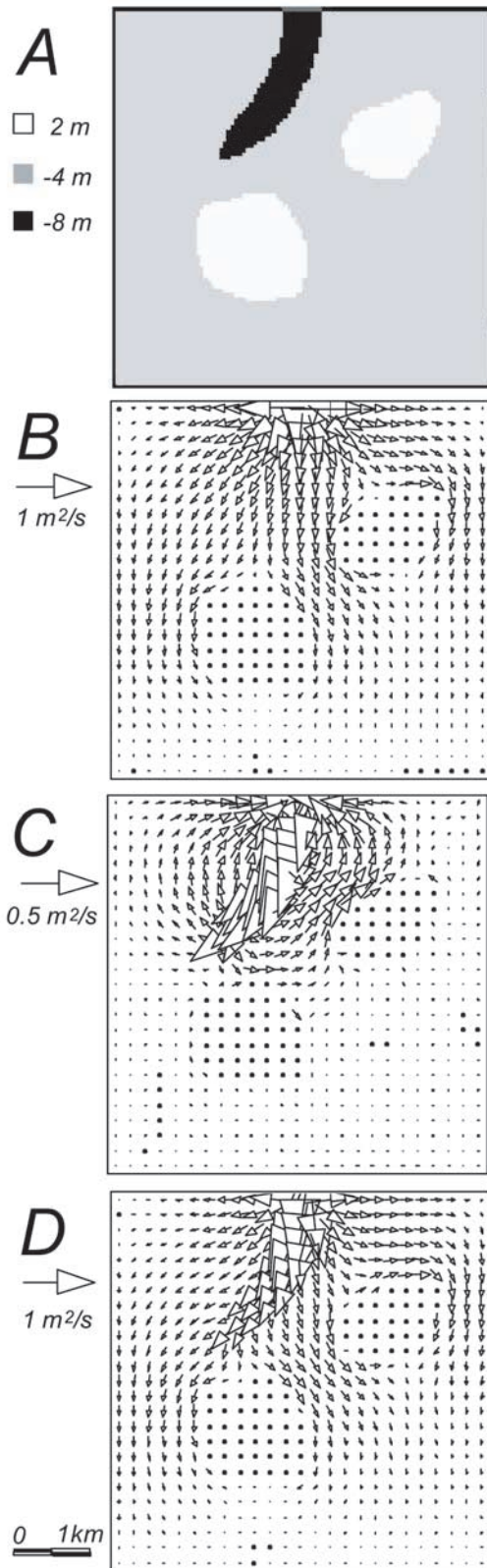


Figure 2. (a) Schematic tidal basin with incised channels and islands. (b) Component of the maximum flood discharge calculated from the potential function. (c) Component of the maximum flood discharge calculated from the stream function. (d) Total maximum flood discharge (sum of the potential and stream solutions).

justifying the application of the present model. Moreover, the phase difference between tides and tidal currents is approximately 90, indicating that the tide is essentially a standing wave [Wang *et al.*, 1998]. The representative parameters for San Diego Bay are $L \approx 16$ km (basin length), $\omega = 1.37 \cdot 10^{-4} s^{-1}$ (semidiurnal tide), $H \approx 5$ m, $C_f \approx 0.0023$, [from Wang *et al.*, 1998]. As a consequence, $\epsilon = 0.015$ and the small embayment hypothesis holds. Since $\Lambda = 7.4$ and $\epsilon\Lambda = 0.11$, we utilize equation (28) instead of equation (21).

[26] The potential function and the stream function can be solved at any instant of the tidal cycle, for each tidal component. Here results for the M2 component when the flood discharge is maximum, (maximum dh_0/dt), are shown. The solution of the potential function is reported in Figure 4a, whereas the corresponding portion of the discharge per unit width is shown in Figure 4b.

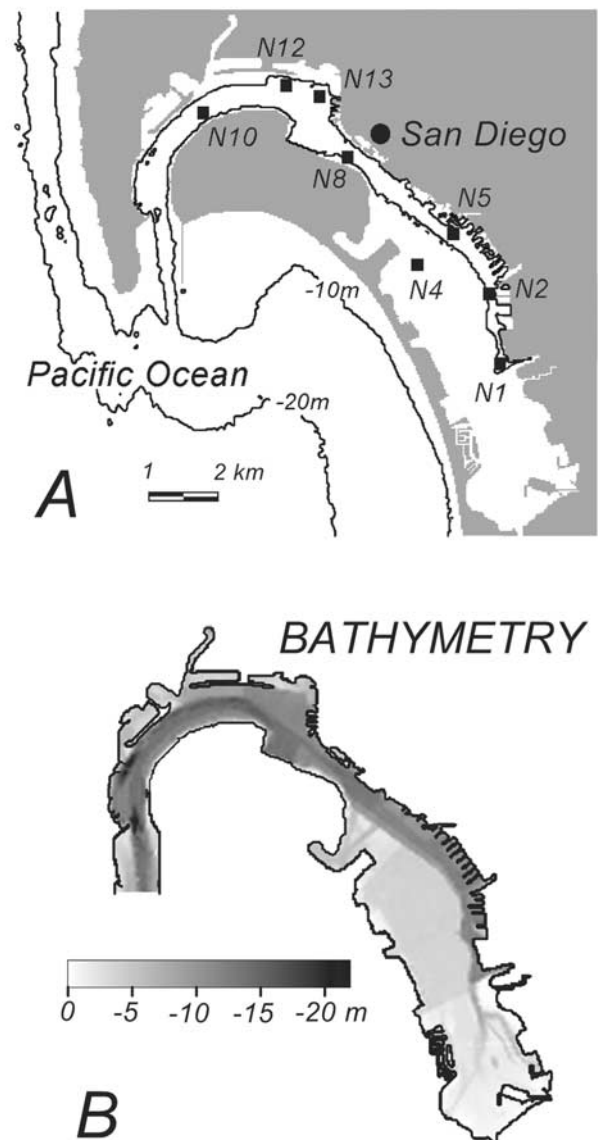


Figure 3. (a) San Diego Bay, California. N1 to N13 are the locations where NOAA collected velocity data in 1983. (b) Bathymetry.

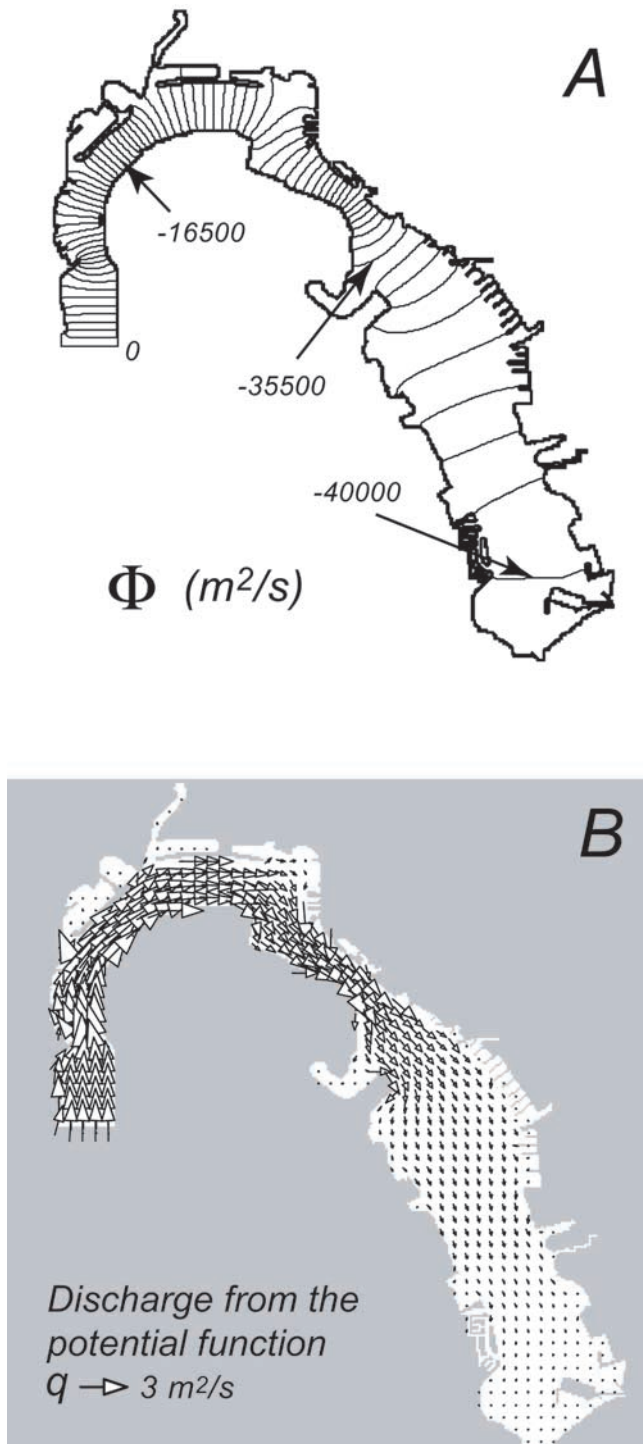


Figure 4. (a) Contour lines for the potential function Φ in San Diego Bay. (b) Component of the maximum flood discharge calculated from the potential function.

[27] The part of the discharge calculated from the potential function has a well-defined distribution. This component decreases from the inlet to the farthest part of the bay, proportionally to the decrease in surface area. The flow is uniformly distributed over bay cross sections, without concentrating in channels. This is because bottom elevation is not considered in the calculation of Φ , and the calculated flow is independent of the water depth.

[28] Once calculated the potential function, the stream function can be derived from equation (28). The boundary condition $\Psi = 0$ on the bay perimeter facilitates the presence of bulges, either with positive or negative value, in the Ψ solution (Figure 5a). At each bulge a circulatory motion is associated, clockwise for positive Ψ , and counterclockwise for negative values (Figure 5b). These “circulations” springing from the stream function solution are responsible for the redistribution of momentum between zones with different depth and discharge, as also indicated by Fagherazzi and Furbish [2001]. When the two solutions derived from Ψ and Φ are added up, the discharge is increased

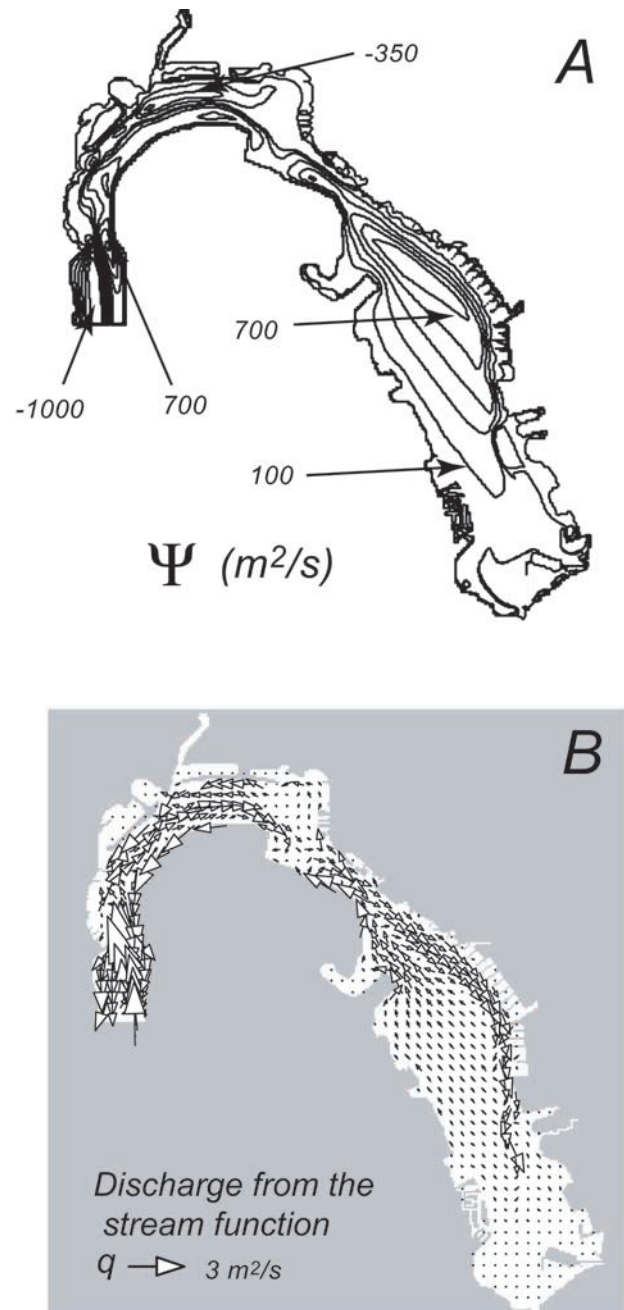


Figure 5. (a) Contour lines for the stream function Ψ in San Diego Bay. (b) Component of the maximum flood discharge calculated from the stream function.

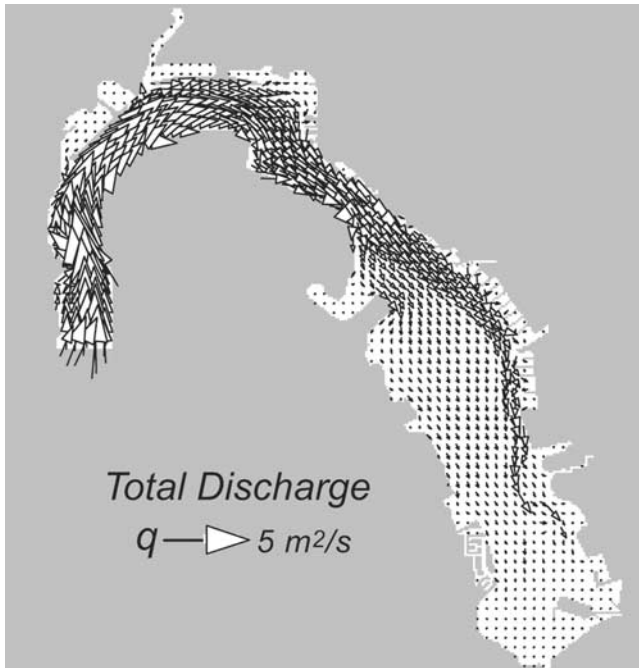


Figure 6. Total maximum flood discharge (sum of the potential and stream solutions).

where the circulation motion derived from Ψ has same direction as the solution derived from Φ and is decreased where the two solutions have opposite direction. Since the stream component of the discharge has zero divergence, the circulations do not change the water balance. In two locations this mechanism is particularly evident. At the inlet, two circulatory motions redistribute the stream component of the discharge from the shallow areas near the banks to the deep central channel. Simultaneously, another circulation of bigger size is present in the southern part of the bay, and it is responsible for flow concentration in the channel in front of the San Diego port. As a conclusion, the total discharge per unit width strongly depends upon bottom topography, with higher discharge in deep areas (Figure 6).

[29] The maximum velocity produced by the model is compared with data collected by NOAA in 11 locations during a tidal current survey conducted in 1983 [Wang *et al.*, 1998]. The M2 and K1 velocity components were extracted with a harmonic analysis, and direction and maximum value calculated [Wang *et al.*, 1998]. Here these data are compared to model simulations for the M2 component (Table 1) and the K1 component (Table 2). For the M2 component, $dh_0/dt_{max} = 7.255 \cdot 10^{-5}$ m/s, whereas for the K1 component $dh_0/dt_{max} = 2.448 \cdot 10^{-5}$ m/s. Where the bottom of the bay is almost uniform (locations N8, N10, and N12; see Figures 3a and 3b), the portion of the discharge derived from the potential function is close to measured values, both in magnitude and direction. Here a 10-m water depth reduces the frictional influence, and the hypothesis of small oscillations with constant depth is probably applicable as a first approximation. In the southern part of the bay, on the other hand, an uneven bottom strongly influences the tidal hydrodynamics. Close to the city port a deep channel carries a large amount of the incoming (outgoing) discharge (Figure 3b). The water is

Table 1. Present Amplitude and Phase Data Both Calculated and Observed for the M2 Tidal Component^a

| Station | Φ | | | $\Phi + \Psi$ | | | Measured | |
|---------|-------------------|-------------|-------------------|-------------------|-------------|-------------------|-------------------|------------------|
| | V_{max} cm/s | Diff., % | Direction, deg | V_{max} cm/s | Diff., % | Direction, deg | V_{max} cm/s | Direction deg |
| N1 | 4.1 | -64 | 150 | 10.1 | -10 | 178 | 11.2 | 179 |
| N2 | 4.2 | -61 | 164 | 12.0 | 11 | 180 | 10.8 | 178 |
| N4 | 19.9 | 70 | 176 | 12.4 | 6 | 176 | 11.7 | 176 |
| N5 | 6.4 | -65 | 135 | 12.5 | -32 | 130 | 18.4 | 134 |
| N8 | 32.9 | -14 | 121 | 39.6 | 4 | 124 | 38.2 | 134 |
| N10 | 27.5 | -6 | 63 | 30.1 | 3 | 63 | 29.2 | 63 |
| N12 | 16.6 | -11 | 101 | 16.7 | -10 | 98 | 18.6 | 106 |
| N13 | 9.8 | -54 | 146 | 13.3 | -27 | 127 | 21.2 | 130 |

^aData reported by Wang *et al.* [1998].

then redistributed from the channel to the shallow areas (depth around 4 m) of the southern bay.

[30] The discharge component calculated from the potential function does not account for the bottom topography, so that the flow entering or leaving the bay is uniformly distributed in the bay cross section. As a consequence, the potential function portion of the discharge overestimates the velocity where the water depth is limited (location N4), and underestimates the velocity in the channel (locations N1, N2, and N5). In this part of the bay, friction is responsible for the concentration of discharge in the channel. When the stream function solution is added to the potential solution, the discharge in the channel increases (locations N1, N2, and N5) whereas the discharge in the tidal flat decreases (location N4) (see Table 1). Moreover, the flow direction over shallow areas changes, from parallel to the channel flow in the weak friction solution (Figure 4b) to oblique to the channel when considering the stream function correction (Figure 6). This behavior is in agreement with measurements in salt marsh environments. In marshes dissected by a channel network [Fagherazzi *et al.*, 1999], the water velocity over the marsh surface is always perpendicular to the channels direction, near the channels banks [Christiansen *et al.*, 2000]. This is due to the high difference in water depths (1–2 m in the channel against a few centimeters on the marsh surface). The correction added by the stream function reduces the difference between calculated and measured values, for both M2 and K1 components (Tables 1 and 2). However, it is important to note that the application of the model to the K1 tidal component produces less precise results, mainly because neglecting the nonlinear inertial terms has a higher influence on secondary tidal components. Finally, it is possible to show from equation (20) that the

Table 2. Present Amplitude and Phase Data Both Calculated and Observed for the K1 Tidal Component^a

| K1 Station | Φ | | | $\Phi + \Psi$ | | | Measured | |
|---------------|-------------------|-------------|-------------------|-------------------|-------------|-------------------|-------------------|------------------|
| | V_{max} cm/s | Diff., % | Direction, deg | V_{max} cm/s | Diff., % | Direction, deg | V_{max} cm/s | Direction deg |
| N1 | 1.4 | -55 | 150 | 3.1 | 0 | 173 | 3.1 | 177 |
| N2 | 1.4 | -79 | 164 | 3.9 | -42 | 189 | 6.7 | 188 |
| N4 | 6.7 | 458 | 176 | 4.2 | 250 | 180 | 1.2 | 219 |
| N5 | 2.2 | -60 | 135 | 4.2 | -24 | 130 | 5.5 | 138 |
| N8 | 11.1 | 32 | 121 | 11.3 | 35 | 152 | 8.4 | 140 |
| N10 | 9.3 | 37 | 63 | 9.9 | 45 | 64 | 6.8 | 70 |
| N12 | 5.6 | -16 | 101 | 5.7 | -15 | 107 | 6.7 | 112 |
| N13 | 3.3 | -60 | 146 | 3.9 | -52 | 127 | 8.1 | 134 |

^aData reported by Wang *et al.* [1998].

total volume of water flowing inside the bay during a half tidal cycle (i.e., the tidal prism) is exactly equal to the volume of water contained between the two horizontal planes corresponding to the maximum and minimum tidal level. In small basins like San Diego Bay where the tide has almost the same amplitude and phase everywhere, the tidal prism calculated by the model is then very close to the real tidal prism. (For San Diego Bay we obtain a tidal prism of $74.8 \times 10^6 \text{ m}^3$ compared to $73 \times 10^6 \text{ m}^3$ reported by Peeling [1975].)

7. Conclusions

[31] In this analysis a simplified model for tidal flow in a basin has been presented. If the dimensions of the basin are small with respect to the tidal wavelength, the assumption of flat water level oscillating synchronously in the whole tidal basin is valid. Under this hypothesis, the discharge per unit width can be decomposed in the sum of two vector fields, respectively governed by a potential function and a stream function. In the shallow water equations the continuity equation then becomes a Poisson equation for the potential function, with suitable boundary conditions. On the other hand, the stream function and corresponding vector field can be calculated from the vorticity equation, once the potential function is known. Both parts of the solution bear a specific meaning. The part of the discharge calculated from the potential function represents the solution for a tidal wave of small amplitude with respect to the water depth, oscillating in a basin with flat bottom. This part of the solution is responsible for the total discharge entering or leaving the basin. The part of the discharge calculated from the stream function, on the other hand, is a correction that has to be added to the potential function solution. The stream function solution redistributes the discharge in the basin as a result of bottom friction, variations in water depth as well as the effect of nonlinear inertial terms. At the same time, the stream function solution does not change the overall volume balance (zero divergence). This study has focused on the effect of friction in momentum redistribution, since for basins with limited depth, inertial terms have a weak influence. In this framework, it is possible to show that the stream function solution is composed by several circulatory motions that transfer momentum from shallow to deep areas. This is particularly valid for basins with channels cutting shallow flats, where most of the water volume is carried by the channel network. The model is tested in San Diego Bay, where the tidal propagation is relatively fast and the tide is essentially a standing wave. The solution extracted from the potential function captures the hydrodynamics of the basin in areas where the bottom is flat, with a reasonable approximation considering the strong simplifications involved. In areas where the water transport mostly occurs in channels, the correction coming from the stream function is necessary in order to increase the predicted flow in the channels and reduce it in the tidal flats. The application of the model to two schematic tidal basins further corroborates the role of the channels in redistributing the discharge within a tidal basin.

[32] **Acknowledgments.** Support for this study was provided by the Office of Naval Research, Geocutter Program, grant N00014-00-1-0822.

We also thank J. Scott Stewart and an anonymous reviewer for the acute suggestions and corrections.

References

- Batchelor, G. K., *An Introduction to Fluid Dynamics*, 615 pp., Cambridge Univ. Press, New York, 1967.
- Boon, J. D., III, Tidal discharge asymmetry in a salt marsh drainage system, *Limnol. Oceanogr.*, 20, 71–80, 1975.
- Bruun, P., *Stability of Tidal Inlets: Theory and Engineering*, 510 pp., Elsevier Sci., New York, 1978.
- Christiansen, T., P. L. Wiberg, and T. G. Milligan, Flow and sediment transport on a tidal salt marsh surface, *Estuarine Coastal Shelf Sci.*, 50, 315–331, 2000.
- Courant, R., and D. Hilbert, *Methods of Mathematical Physics*, Wiley-Intersci., New York, 1953.
- Fagherazzi, S., Basic flow field in a tidal basin, *Geophys. Res. Lett.*, 29(8), 1221, doi:10.1029/2001GL013787, 2002.
- Fagherazzi, S., and D. J. Furbish, On the shape and widening of salt-marsh creeks, *J. Geophys. Res.*, 106(C1), 991–1003, 2001.
- Fagherazzi, S., A. Bortoluzzi, W. E. Dietrich, A. Adami, S. Lanzoni, M. Marani, and A. Rinaldo, Tidal networks, 1, Automatic network extraction and preliminary scaling features from digital elevation maps, *Water Resour. Res.*, 35(12), 3891–3904, 1999.
- Friedrichs, C. T., and D. G. Aubrey, Tidal propagation in strongly convergent channels, *J. Geophys. Res.*, 99(C2), 3321–3326, 1994.
- Friedrichs, C. T., and O. S. Madsen, Nonlinear diffusion of the tidal signal in frictionally dominated embayments, *J. Geophys. Res.*, 97(C4), 5637–5650, 1992.
- Healey, R. G., K. Pye, D. R. Stoddart, and T. P. Bayliss-Smith, Velocity variation in salt marsh creeks, Norfolk, England, *Estuarine Coastal Shelf Sci.*, 13, 535–545, 1981.
- Jeffreys, H., and B. Swirles, *Methods of Mathematical Physics*, Cambridge Univ. Press, New York, 1972.
- Lanzoni, S., and G. Seminara, On tide propagation in convergent estuaries, *J. Geophys. Res.*, 103(C13), 30,793–30,812, 1998.
- LeBlond, P. H., Tidal propagation in shallow rivers, *J. Geophys. Res.*, 83, 4717–4721, 1978.
- Pedlosky, J., *Geophysical Fluid Dynamics*, 710 pp., Springer-Verlag, New York, 1987.
- Peeling, T. J., A proximate biological survey of San Diego Bay, California, Rep. TP389, Naval Undersea Cent., San Diego, Calif., 1975.
- Pethick, J. S., Velocity surges and asymmetry in tidal channels, *Estuarine Coastal Mar. Sci.*, 11, 331–345, 1980.
- Prandle, D., Tides in estuaries and embayments (review), in *Tidal Hydrodynamics*, edited by B. B. Parker, pp. 125–152, John Wiley, New York, 1991.
- Rinaldo, A., S. Fagherazzi, S. Lanzoni, M. Marani, and W. E. Dietrich, Tidal networks, 2, Watershed delineation and comparative network morphology, *Water Resour. Res.*, 35(12), 3905–3917, 1999a.
- Rinaldo, A., S. Fagherazzi, S. Lanzoni, M. Marani, and W. E. Dietrich, Tidal networks, 3, Landscape-forming discharges and studies in empirical geomorphic relationships, *Water Resour. Res.*, 35(12), 3919–3929, 1999b.
- Schuttelaars, H. M., and H. E. de Swart, An idealized long-term morphodynamic model of a tidal embayment, *Eur. J. Mech. B-Fluid*, 15(1), 55–80, 1996.
- Schuttelaars, H. M., and H. E. de Swart, Initial formation of channels and shoals in a short tidal embayment, *J. Fluid Mech.*, 386, 15–42, 1999.
- Schuttelaars, H. M., and H. E. de Swart, Multiple morphodynamic equilibria in tidal embayments, *J. Geophys. Res.*, 105(C10), 24,105–24,118, 2000.
- Stoker, J. J., *Water waves, the Mathematical Theory With Applications*, 567 pp., Wiley-Intersci., New York, 1957.
- Velyan, T., *Shallow Water Hydrodynamics*, *Oceanogr. Ser.*, vol. 55, 434 pp., Elsevier Sci., New York, 1992.
- Wang, P. F., R. T. Cheng, K. Richter, E. S. Gross, D. Sutton, and J. W. Gartner, Modeling tidal hydrodynamics of San Diego Bay, California, *J. Am. Water Resour. Assoc.*, 34(5), 1123–1140, 1998.
- Wright, J., C. Angela, and D. Park (Eds.), *Waves, Tides and Shallow-Water Processes*, 227 pp., Open Univ., Butterworth-Heinemann, Woburn, Mass., 2000.
- Zimmerman, J. T. F., Topographic generation of residual circulation by oscillatory (tidal) currents, *Geophys. Astrophys. Fluid Dyn.*, 11, 35–47, 1978.

S. Fagherazzi, Computational Science and Information Technology Florida State University, Dirac Science Library, Tallahassee, FL 32306-4120, USA. (sergio@csit.fsu.edu)

A. D. Howard and P. L. Wiberg, Department of Environmental Sciences, University of Virginia, P.O. Box 400123, Charlottesville, VA 22904-4123, USA. (ah6p@virginia.edu; pw3c@humboldt.evsc.virginia.edu)